Electrical Power and Energy Systems 33 (2011) 1172–1184

Contents lists available at ScienceDirect

Electrical Power and Energy Systems

journal homepage: www.elsevier.com/locate/ijepes

Impact of FACTS controllers on the stability of power systems connected with doubly fed induction generators

N. Senthil Kumar *, J. Gokulakrishnan

Department of Electrical and Electronics Engineering, B.S. Abdur Rahman University (Formerly B.S.A. Crescent Engineering College), GST Road, Vandalur, Chennai, Tamilnadu, India

ARTICLE INFO

Article history:
Received 16 April 2008
Received in revised form 7 January 2011
Accepted 28 January 2011
Available online 30 March 2011

Keywords:
Wind energy conversion systems
Doubly fed induction generators
Flexible alternating current transmission systems
Rotor angle stability
Rotor speed stability

ABSTRACT

The increasing power demand has led to the growth of new technologies that play an integral role in shaping the future energy market. Keeping in view of the environmental constraints, grid connected wind turbines are promising in increasing system reliability. This paper presents the impact of FACTS controllers on the stability of power systems connected with wind energy conversion systems. The wind generator model considered is a variable speed doubly fed induction generator model. The stability assessment is made first for a three phase short circuit without FACTS controllers in the power network and then with the FACTS controllers. The dynamic simulation results yield information on (i) the impact of faults on the performance of induction generators/wind turbines, (ii) transient rating of the FACTS controllers for enhancement of rotor speed stability of induction generators and angle stability of synchronous generators. EUROSTAG is used for executing the dynamic simulations.

1. Introduction

As power systems became interconnected, areas of generation were found to be prone to electromechanical oscillations. These oscillations have been observed in many power systems worldwide. As the level of power transmission rose, largely through existing interconnections, which were becoming relatively weak and inadequate, load characteristics added to the problem causing spontaneous oscillations. The oscillations may be local to a single generator or generator plant (local oscillations, 1.0–2 Hz), or they may involve a number of generators widely separated geographically (interarea oscillations 0.2–0.8 Hz). If not controlled, these oscillations may lead to total or partial power interruption [1]. Wind energy development is consumer and environment friendly, requires shorter construction time and is cost competitive. It becomes one of the most competitive sources of renewable energy. However, wind power has some disadvantages. Mostly, wind powered generators are induction generators. The induction generator absorbs reactive power during its normal operating condition. This may create low voltage and dynamic instability in the system [2]. There are two major types of wind generator models, which are used very widely. The first one is the squirrel cage induction generator and the second one doubly fed induction generator. For the present work doubly fed induction generator model is used for executing dynamic simulations as they possess several advantages than fixed speed induction generators which are (i) advanced energy capture (ii) improved power quality and (iii) reduced mechanical stress. The dynamic stability of a single wind turbine generator supplying an infinite bus through a transmission line was studied by developing the linearized model of the power system under different loading conditions [3]. The effect of wind turbines on the transient fault behavior of the nordic power system was investigated for different faults in [4]. A new definition on rotor speed stability of fixed speed induction generators is proposed in [5]. This manuscript examines the dynamic behavior of the doubly fed induction generator in line with Ref. [5]. The impact of high wind power penetration on power system oscillation stability is investigated in [6]. The effect of wind power on the oscillations is investigated by gradually replacing the power generated by the synchronous generators in the system by power from either constant or variable speed turbines.

An efficient reduced order model of DFIG is proposed for rotor and grid side converters for all the four operating modes in [7]. The rotor current controller model developed in Ref. [7] is used to control the DFIG in this paper. The application of voltage source converter (VSC) based transmission controllers for wind energy conversion systems are discussed in [8]. The application of a STATCOM with battery energy storage to smooth the line power of wind farm consisting of a fixed speed wind farm was discussed in Ref. [9]. The modeling of large offshore wind farms for voltage stability analysis using PSS/E and voltage stability enhancement using SVC was discussed in [10]. The dynamic behavior of DFIG and the effect of fault ride through of DFIG wind turbines are studied in [11]. The dynamic behavior of DFIG wind turbines during grid faults is simulated and assessed using the DIgSILENT.

* Corresponding author.
E-mail address: senthilkumarsaieshwar@gmail.com (N. Senthil Kumar).

0142-0615/$ - see front matter © 2011 Elsevier Ltd. All rights reserved.
doi:10.1016/j.ijepes.2011.01.031

The objective of the present work is to study the impact of FACTS controllers on the dynamic performance of the power system connected with a doubly fed induction generator to the wind farm. The dynamic stability of the system is studied by running time domain simulations using the EUROSTAG software [12] with and without FACTS controllers. The following FACTS controllers are taken up for the dynamic analysis.

(i) Static var compensator (SVC).
(ii) Static compensator (STATCOM).
(iii) Thyristor controlled series capacitor (TCSC).
(iv) Unified power flow controller (UPFC).

This paper is organized as follows Section 2 presents the modeling of power system and wind turbine along with FACTS controllers. Section 3 presents the dynamic simulation results obtained for a three phase transient fault on the system with and without FACTS controllers. Section 4 presents results and discussion on the simulation results obtained. Section 5 presents the conclusion.

2. Modeling of the power system and wind turbine

In general for the purpose of dynamic analysis power systems are modeled by a set of differential and algebraic equations (DAE), that is:

$$\begin{aligned} \dot{x} &= f(x, y, \lambda, p) \\ 0 &= g(x, y, \lambda, p) \end{aligned} \tag{1}$$

where $x \in R^n$ is a vector of state variables associated with the dynamic states of generators, loads and other system controllers. $y \in R^m$ is a vector of algebraic variables associated with steady state variables resulting from neglecting fast dynamics (e.g., most load voltage phasor magnitudes and angles); $\lambda \in R^l$ is a set of uncontrollable parameters, such as variations in active and reactive power of loads; $p \in R^k$ is a set of controllable parameters such as transformer tap, AVR settings and FACTS controller reference voltages.

2.1. Wind turbine concepts and modeling

Normally a wind turbine creates mechanical torque on a rotating shaft, while an electrical generator on the same rotating shaft is controlled to produce an opposing electromagnetic torque. The power and torque equations for the wind turbine are as follows:

$$P = (\rho/2)^* C_p(\lambda, \theta) A V^3 \tag{2}$$

$$T_m = \frac{P}{\omega} \tag{3}$$

where ρ is the density of air (1.22 kg/m^3); A is the swept area of the blade in m^2. C_p is the performance co-efficient which represents the rotor efficiency of the turbine (captured power/wind power); V is the wind speed (m/s); P is the output power of the turbine; ω is the rotor speed of wind turbine; λ is the tip speed ratio V_t/V, the ratio between blade tip speed V_t and wind speed upstream the rotor V (m/s); θ is the pitch angle in degrees.

The parameters of the modeled system are given in the Appendix.

The wind turbine and its associated controls are modeled using the EUROSTAG software [12] (Tractable Engineering, 2004) and the main control units modeled are shown in Fig. 1. The main controller manages the overall control functions, whereas pitch and power controller are subordinate units.

The wind energy conversion scheme used for simulation consists of a doubly fed induction generator (rotor circuit connected to the grid through power electronic converter). The converter adjusts the frequency of the rotor feeding current to enable variable speed operation (Fig. 2).

2.2. Doubly fed induction generator model

The doubly fed induction generator is the most commonly used machine for wind power generation. The rotor terminals are fed with a symmetrical three-phase voltage of variable frequency and amplitude. Using the generator convention, the following set of dynamic equations results:

$$V_{ds} = -R_s i_{ds} - \omega_s \psi_{qs} + d\psi_{ds}/dt \tag{4}$$

$$V_{qs} = -R_s i_{qs} + \omega_s \psi_{ds} + d\psi_{qs}/dt \tag{5}$$

$$V_{dr} = -R i_{dr} - s\omega_s \psi_{qr} + d\psi_{dr}/dt \tag{6}$$

$$V_{qs} = -R_r i_{qr} + s\omega_s \psi_{dr} + d\psi_{qr}/dt \tag{7}$$

where v is the voltage in (V), R is the resistance in (Ω), i the current in (A) and ω_s the stator electrical frequency in (rad/s), ψ the flux linkage (Vs) and s the rotor slip [13].

From the above set of dynamic equations d and q indicate the direct and quadrature axis components and s and r indicate stator and rotor quantities. The d–q reference frame is rotating at

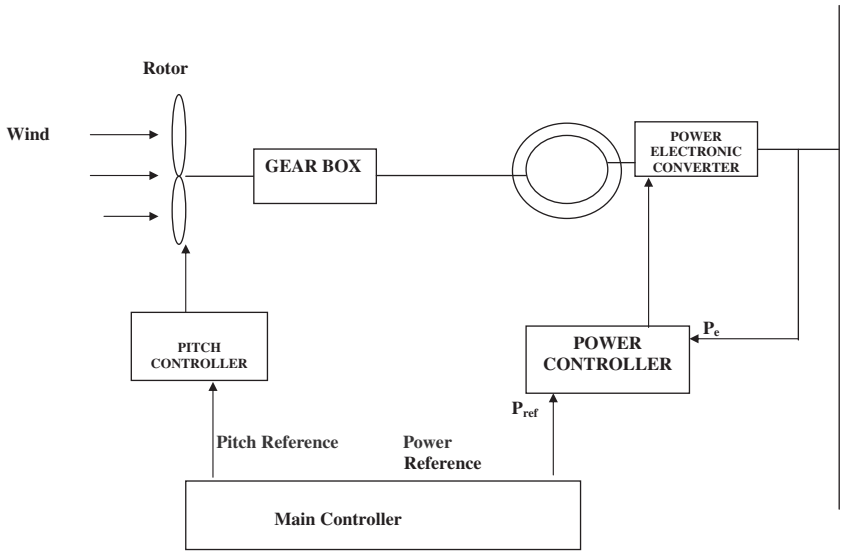

Fig. 1. Wind energy conversion scheme and its associated controls.

synchronous speed with the q-axis 90° ahead of the d-axis.The flux linkages in Eq. (7) can be calculated using the following set of equations in per unit:

$$\begin{aligned}\psi_{ds} &= -(L_s + L_m)i_{ds} - L_m i_{dr}\\ \psi_{qs} &= -(L_s + L_m)i_{qs} - L_m i_{qr}\\ \psi_{dr} &= -(L_r + L_m)i_{dr} - L_m i_{ds}\\ \psi_{qr} &= -(L_r + L_m)i_{qr} - L_m i_{qs}\end{aligned} \tag{8}$$

with L_m is the mutual inductance and L_s and L_r, are the stator and rotor leakage inductances respectively in (8).

The changes in generator speed that result from a difference in electrical and mechanical torque can be calculated using generator equation of motion

$$\frac{d\omega_s}{dt} = \frac{1}{2H}(T_m - T_e) \tag{9}$$

where H is the inertia constant (seconds) and T_m is the mechanical torque.

T_e is the electro mechanical torque generated by the DFIG:

$$T_e = \psi_{dr} i_{qr} - \psi_{qr} i_{dr} \tag{10}$$

The converters are represented as current sources, and therefore the current set points equal rotor currents. The current set points are derived from the set points for active and reactive power. The active power set point is generated by the rotor speed controller, based on the actual rotor speed value. The reactive power set point is generated by the terminal voltage controller or power factor controller, based on the actual value of the terminal voltage or the power factor.

2.3. Synchronous generators

The synchronous generator model used for this dynamic analysis is the two axis model with four state variables [14]:

$$\begin{aligned}\dot{E}'_{di} &= \frac{1}{\tau'_{qoi}}(-E'_{di} - (x_{qi} - x'_{qi})I_{qi})\\ \dot{E}'_{qi} &= \frac{1}{\tau'_{doi}}(E_{FDi} - E'_{qi} + (x_{di} - x'_{di})I_{di})\\ \dot{\omega}_i &= \frac{1}{\tau_{ji}}(T_{mi} - D\omega_i - T_{ei})\\ \dot{\delta}_i &= \omega_i\\ i &= 1, 2, \ldots, n\end{aligned} \tag{11}$$

where the state variables are E'_d is the direct axis component of voltage behind transient reactance, E'_q is the quadrature axis component of voltage behind transient reactance, ω is the angular velocity of rotor, δ is rotor angle

2.4. Static var compensators (SVC)

SVC is basically a shunt connected static var generator/absorber whose output is adjusted to exchange capacitive or inductive current so as to maintain or control specific power system variables;

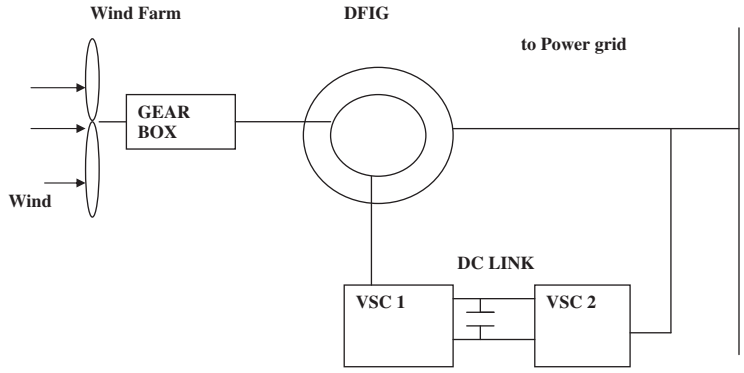

Fig. 2. Structure of the doubly fed Induction generator based wind turbine system.

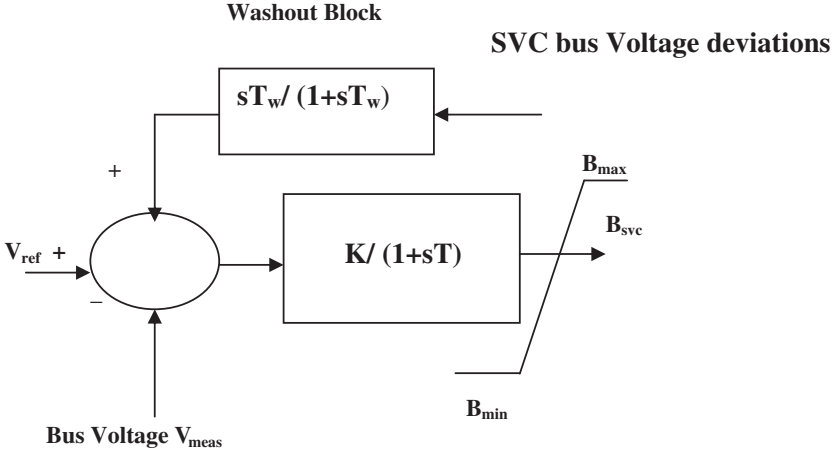

Fig. 3. Structure of SVC controller with stabilizing loop.

typically, the controlled variable is the SVC bus voltage. One of the major reasons for installing an SVC is to improve dynamic voltage control, and thus, increase system loadability. An additional stabilizing signal, and supplementary control superimposed on the voltage control loop of an SVC can provide damping of system oscillations during transient faults and disturbances (Fig. 3) [16]. The state equation for SVC can be written as:

$$B_{SVC} = \frac{K}{T}(V_{ref} - V_{meas} + u) - \frac{1}{T}B_{SVC} \tag{12}$$

where B_{SVC} the SVC susceptance, u is the stabilizing loop output.

Here, V_{ref} is chosen as 1.0 per-unit and V_{meas} is the PCC voltage.

2.5. STATCOM

The STATCOM resembles in many respects a synchronous compensator, but without inertia. The basic electronic block of a STATCOM is the voltage source converter (VSC), which in general converts an input dc voltage into a three-phase output voltage at fundamental frequency, with rapidly controllable amplitude and phase. α is the phase shift between the controller VSC AC voltage and its bus voltage V. V_{ref} is the reference voltage setting.[15]

The dynamic equations include the differential equations for the voltage magnitude controller, phase angle controller and STATCOM power balance. The following differential equations (in per-unit) can be written from the block diagrams given in Figs. 4a and 4b:

$$V_x = \frac{[K_{M_{ac}}V - V_x]}{T_{M_{ac}}} \tag{13}$$

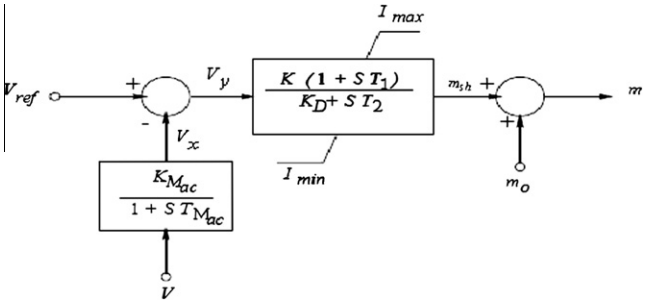

Fig. 4a. PWM voltage magnitude controller of STATCOM.

$$m_{sh} = \frac{[kV_y + KT_1 V_y - K_D m_{sh}]}{T_2} \tag{14}$$

$$V_{dcx} = \frac{[K_{M_{dc}}V_{dc} - V_{dcx}]}{T_{M_{dc}}} \tag{15}$$

$$\Delta\alpha = K_P V_{dcy} + K_I V_{dcy} \tag{16}$$

where, V_x is the output of AC voltage measuring circuit; V_{dcx} is output of DC voltage measuring circuit; $\Delta\alpha$ is the output of phase angle controller block; m_{sh} can be obtained from, $K_{M_{ac}}$ and $T_{M_{ac}}$ are the gain and time constant of the ac voltage measuring circuit respectively. V_{dcy} is the input to the PI controller in DC voltage measuring circuit.

$$k = \sqrt{\frac{3}{8}}(m_0 + m_{sh}) \tag{17}$$

Here, k is the proportionality constant of STATCOM PWM VSC output voltage and

$$m_0 = \sqrt{\frac{8}{3}}\left(\frac{V_{ref}}{V_{dc}}\right) \tag{18}$$

2.6. Thyristor controlled series capacitors (TCSC)

Thyristor controlled series capacitor schemes typically use a thyristor controlled reactor in parallel with a capacitor to vary the effective compensating reactance. For the purpose of analysis, the TCSC, regardless of its practical implementation, can be considered simply as a continually variable capacitor whose reactance is controllable in the range of $0 \leqslant X_c \leqslant X_{cmax}$. The single line diagram of the TCSC is shown in Fig. 5. The variable reactance model of TCSC is as shown in Fig. 6. The reference value of the TCSC reactance X_{ref} is fixed based on the degree of compensation required. For the present work the value of X_{ref} is chosen as half of the line inductive reactance. X_C is the variable reactance inserted by the TCSC module into the line [16].

$$X_C = \frac{(X_{ref} - X_{meas} + U)K - X_C}{T} \tag{19}$$

X_{ref} is the reference value of TCSC reactance to be inserted in the line; X_{meas} is the measured reactance; U is the stabilizing signal; T is the time constant of the controller; X_{max} and X_{min} is the maximum and minimum limits of reactance.

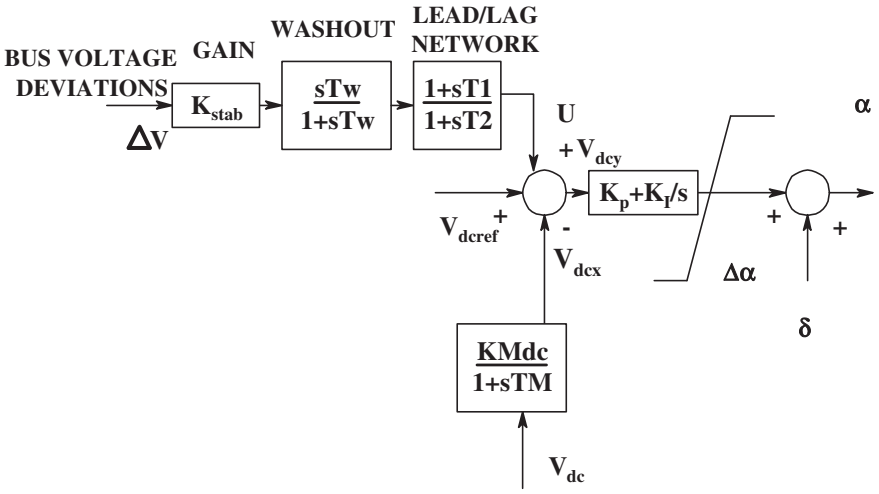

Fig. 4b. PI phase angle controller for STATCOM.

2.7. Unified power flow controllers (UPFC)

The UPFC is the most versatile FACTS controller developed so far, with all encompassing capabilities of voltage regulation, series compensation, and phase shifting. It comprises of two voltage source converters coupled through a common DC link. The single line diagram is shown in Fig. 7.

The active and reactive power flow control loops of the UPFC is shown in Figs. 8 and 9. The stabilizing signal for the unified power flow controller is derived from a power oscillation-damping block, which uses active power flow (P_{flow}) as the input signal. $P_{flow\ Ref}$ is the reference value of active power flow in the line on which UPFC is connected. This value is obtained after running a power flow in the line on which UPFC is to be connected. V_{seq} is the component of series injected voltage in quadrature with the line current. Q_{ref} is the reference setting for reactive power flow in the UPFC connected line and Q_{flow} is the actual reactive power flow in the line and V_{sep} is the component of AC voltage injected in phase with the line current.

2.7.1. Parameter tuning of FACTS controllers

The parameter tuning of FACTS controllers is an important problem as the stabilizing effect will depend on the gain of the controllers. The tuning is posed as an optimization problem with the objective as minimizing the oscillations of PCC voltage from the desired value and is given by:

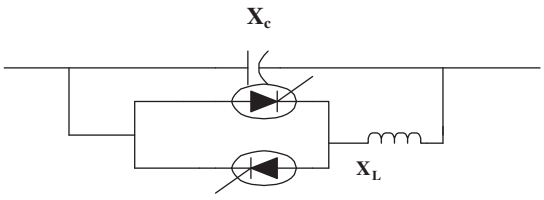

Fig. 5. Thyristor controlled series capacitor.

$$\text{Minimize}: PI = \sum_{k}[(V_{ref} - V_k)^2 + (\omega_{ref} - \omega_k)^2] \quad (20)$$

$$K_{min} \leqslant K \leqslant K_{max}$$

where V_{ref} = 1.0 per-unit and PI is the sum squared deviation index of the PCC voltage.

The optimization problem is solved using sequential quadratic programing in MATLAB.

3. Dynamic simulation results and stability investigation

The single line diagram of the test system with the wind turbine connected is shown in Fig. 10. The test system consists of a six bus system with two synchronous generators G1 and G2. The doubly fed induction generator (IG) is connected to the grid through a two winding transformer. IG denotes the induction generator terminal node. The two synchronous generators are rated at 1100 MW (G1) and 5500 MW (G2). The wind farm is represented by an aggregated model consisting of 10 wind turbines of each 2 MW. The induction generator is injecting 5.5 MW in the steady state. The total system load at bus 4 and 5 is 1500 MW which corresponds to nominal operating condition.

5 and 4 are load buses. At bus 5 the load is represented as a combination of Impedance and voltage frequency dependant load in the dynamic simulation. The dynamic simulation is carried out for a three phase fault on line 1–2 in the second line. The three phase fault is cleared in five cycles. The shunt connected FACTS controllers (SVC and STATCOM) are located near bus 2 and the series connected FACTS controllers are located in one of the 2–3 lines.

3.1. Rotor angle deviations of synchronous generators without wind farm, with wind farm and with FACTS controllers

Fig. 11 shows the rotor angle response of the synchronous generators without the wind farm in the network. From Fig. 11 it can

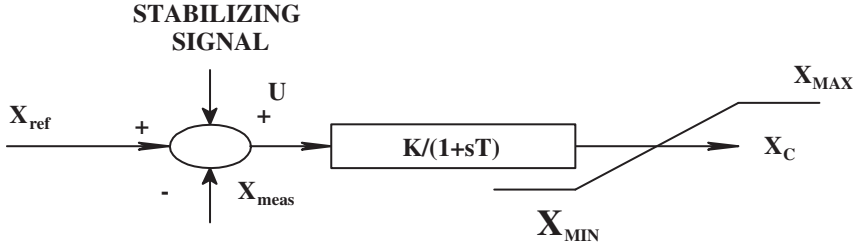

Fig. 6. Dynamic model of TCSC.

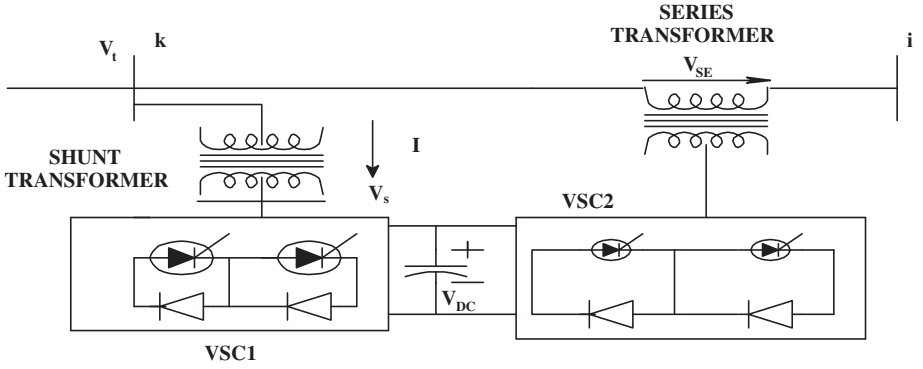

Fig. 7. Single line diagram of UPFC.

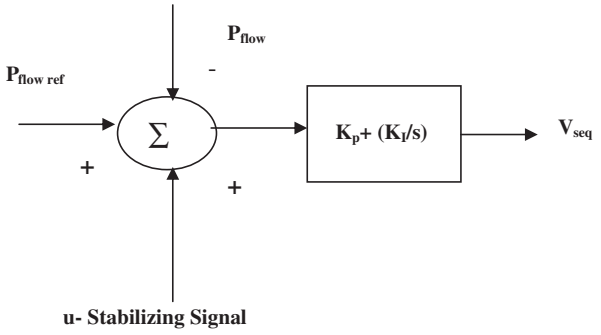

Fig. 8. Active power flow control loop.

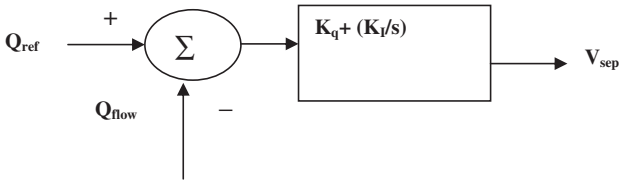

Fig. 9. Reactive power flow control loop.

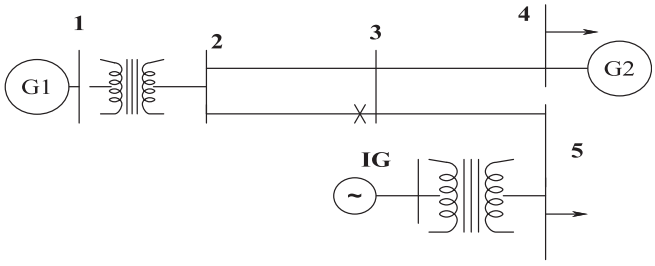

Fig. 10. Single line diagram of the power system with DFIG.

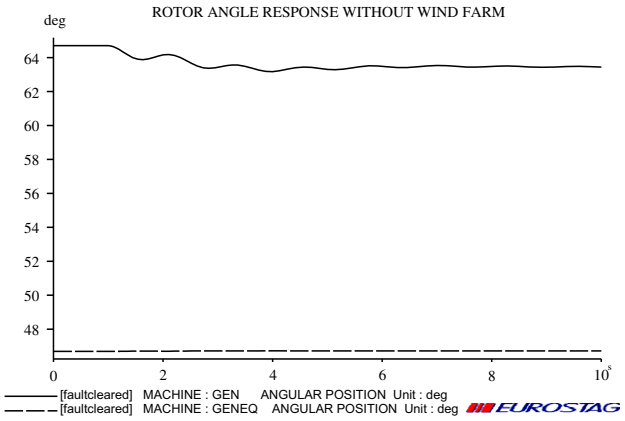

Fig. 11. Rotor angle response without wind farm.

be observed that after the fault the generator rotor angle of G1 deviates slightly but after the fault clearance the system returns to a new post equilibrium rotor angle value. Generator G2, which supplies a local load, lies far away from the transient fault and hence is left unperturbed. Fig. 12 shows the rotor angle response of the synchronous generators with wind farm included in the network.

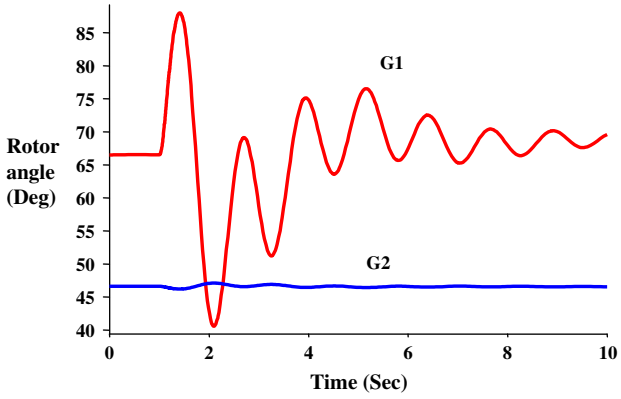

Fig. 12. Rotor angle response with wind farm – High load operating condition.

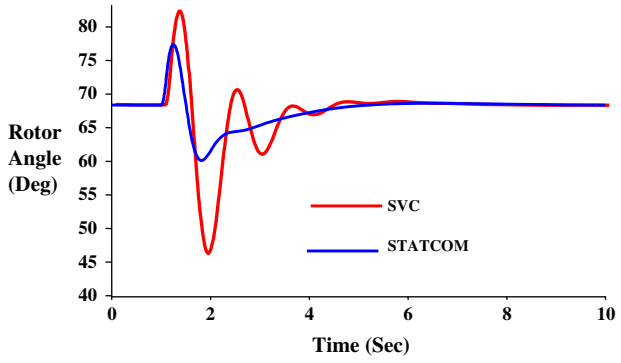

Fig. 13. Rotor angle response of synchronous machine G1 with wind farm – Effect of SVC and STATCOM – High load operating condition.

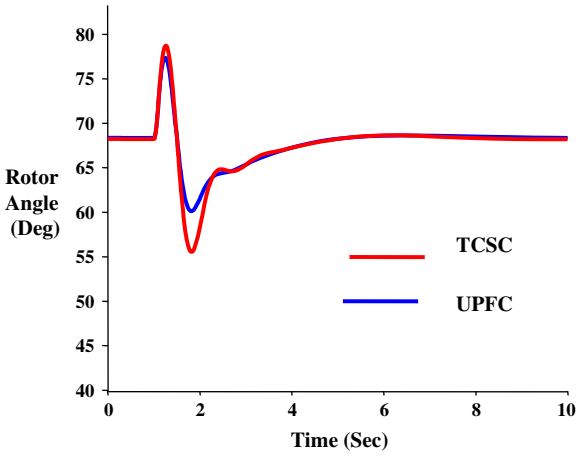

Fig. 14. Rotor angle response of synchronous machine G1 with wind farm – Effect of TCSC and UPFC – High loading condition.

From Fig. 12 it can be observed that the rotor angle of synchronous generator G1 oscillates indefinitely. This leads to dynamic instability (sustained oscillations of rotor angle) in the system. Figs. 13 and 14 show the rotor angle response of synchronous generators with shunt and series controllers included in the transmission line network. Responses shown in Figs. 13 and 14 correspond to the high load operating condition where the total system load is increased by 40%. The controller parameters of the static var compensator/STATCOM are tuned to stabilize the oscillations as given by the objective function of Eq. (12).

From Fig. 13 it can be observed that rotor angle oscillations settle down after 4 s with the SVC controller included in the network. The oscillations settle down in 2 s with STATCOM.

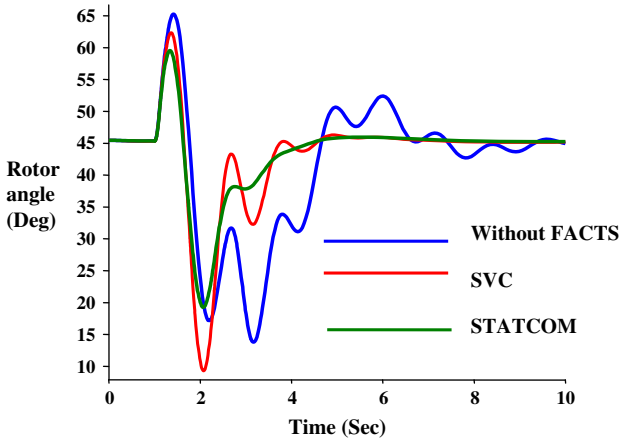

Fig. 15. Rotor angle response of synchronous machine G1 with wind farm – Effect of SVC and STATCOM – Nominal loading condition.

This may be attributed due to the fact that STATCOM (A voltage source converter based FACTS controller) has a faster transient response compared to static var compensator (a passive thyristor switched reactor/capacitor). From Fig. 14 it can be observed that there are no oscillations in the rotor angles of synchronous generator with UPFC in the network. Figs. 15 and 16 shows the rotor angle response of synchronous generators with shunt and series controllers in the network when the system load level is at its nominal value as specified in Section 3.

The parameters of both TCSC and UPFC controllers are optimized to enhance system damping. From Fig. 15 it can be observed that the rotor angle oscillations settle down in 7 s and with UPFC (Fig. 16) the oscillations settle down in 5 s. This is due the fact that UPFC contributes reactive power to the network after the disturbance from its shunt branch.

3.2. Rotor speed deviation of DFIG – Effect of FACTS controllers

Fig. 17a demonstrates the effect of FACTS devices on the rotor speed response of DFIG after the disturbance. The speed of the induction generator tends to increase towards its maximum value set (1.2 per-unit) in the dynamic simulation without FACTS controllers in the network After the clearance of the fault it is observed that the speed of the wind turbine does not reach its prefault stea-

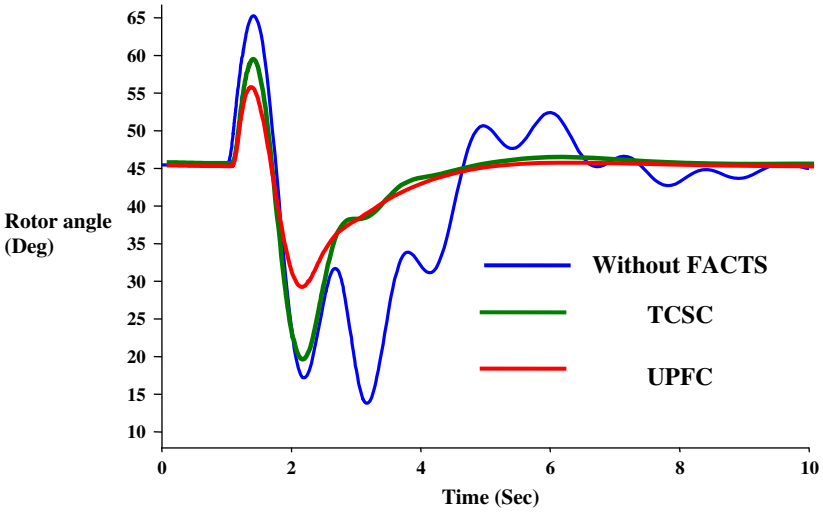

Fig. 16. Rotor angle response of synchronous machine G1 with wind farm – Effect of TCSC and UPFC – Nominal operating condition.

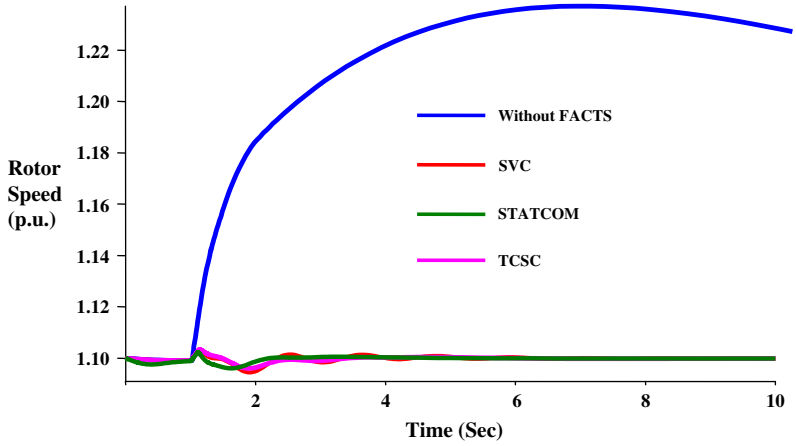

Fig. 17a. Rotor speed response of DFIG – Effect of FACTS devices. High load operating condition.

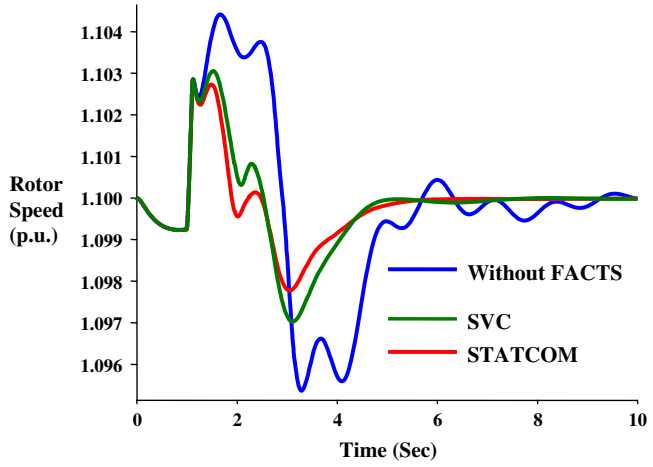

Fig. 17b. Rotor speed response of DFIG – Effect of FACTS devices nominal operating condition.

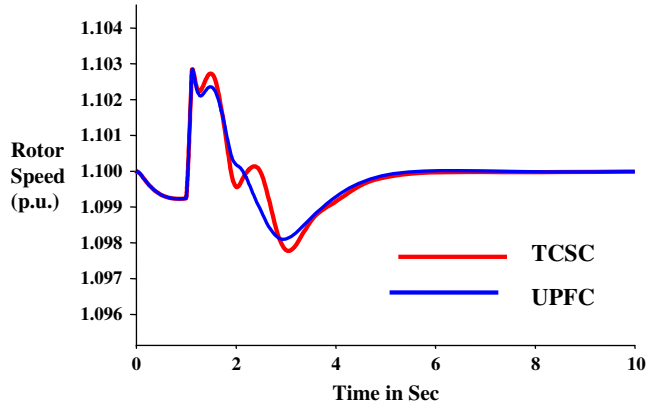

Fig. 17c. Rotor speed response of DFIG – Effect of FACTS devices nominal operating condition.

dy state value of 1.1 p.u. This post fault rotor speed deviation of the asynchronous generator causes rotor speed instability as discussed in Ref. [6].

However with the SVC additional dynamic reactive power support and the stabilizing signal provided suppresses the rotor speed oscillations of the asynchronous generators. From Figs. 17a–17d it can be inferred that there are no appreciable speed deviations with UPFC controller in the network. This is due to the effectiveness of UPFC damping controller attached with its power flow controller and also due to the shunt reactive support provided by the UPFC (Figs. 8 and 9). Hence it can be concluded that UPFC damps out rotor speed/rotor angle oscillations of asynchronous and synchronous generators more effectively. The impact of FACTS controllers on the rotor speed stability following the outage of generator G1 is shown in Fig. 17(d), with and without SVC in the network.

The effect of the fault ride through attached with rotor side converter of DFIG has a very minimal effect following a contingency (generator outage) which causes the rotor speed of the induction generator to deviation from its steady state.

3.3. Active power injected by the DFIG – Effect of FACTS controllers

Fig. 18 shows the active power injected by the wind turbine into the grid following the three phase fault carried on one of the lines near bus 3. The stator protection system associated with the induction generator disconnects the stator from the grid if the terminal voltage of the induction generator is less than 0.75 p.u. for a period of 0.08 s, hence the stator active power delivered comes down to zero after the fault. The active power injected comes down to zero from its initial value of 5.5 MW specified in the load flow.

The power calculation according to Eq. (2) is based on a single wind speed. However, in reality, the wind speed may differ slightly in direction and intensity across the area traversed by the blades. To consider this effect, the wind speed is supplied through a lag block to the power conversion equation. This creates a slight change in the active power delivered to the grid before the disturbance at 1 s. Fig. 19 shows the wind speed block given as input to the algebraic equation of power. [7].

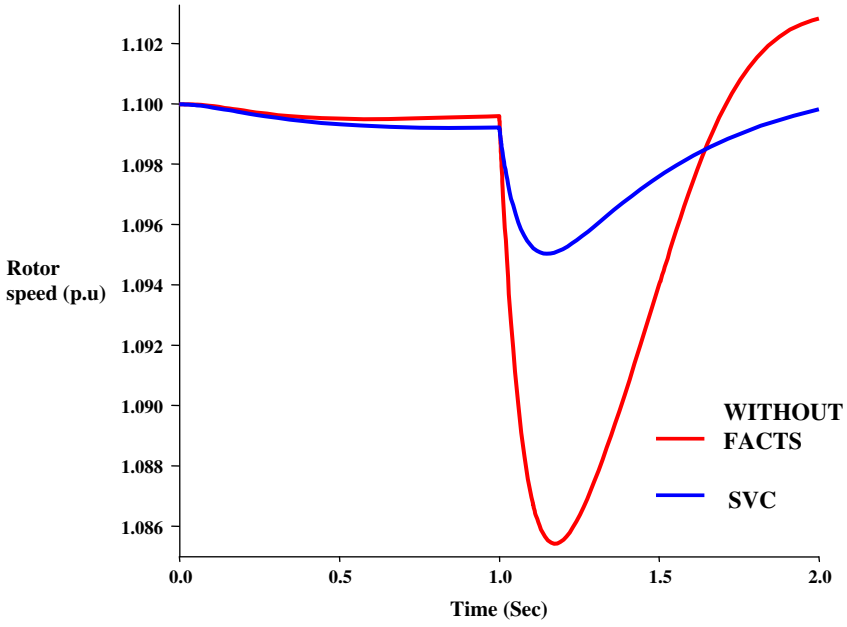

Fig. 17d. Effect of rotor speed stability following the outage of Synchronous generator G1 with and without SVC.

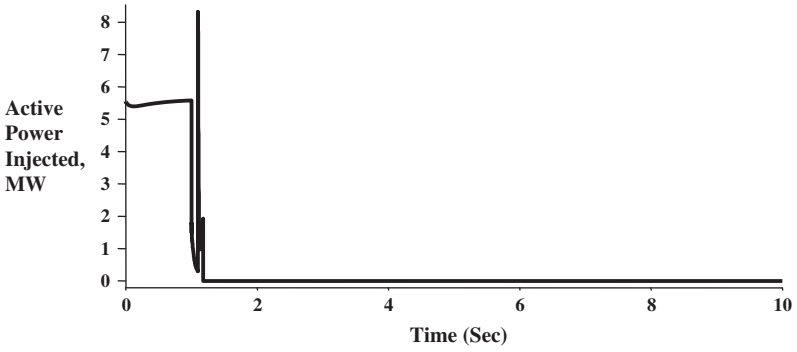

Fig. 18. Active power Injected by the wind farm without FACTS devices.

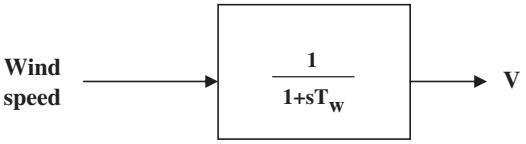

Fig. 19. Wind speed supplied through lag block.

Fig. 20 shows the active power injected by the wind turbine into the grid following the transient fault with SVC/TCSC. It can be observed that after the fault the active power injected oscillates around the steady state power injection value of 5.5 MW and the MW injection into the grid does not become zero with SVC. This is due to the dynamic reactive power support provided by the SVC/TCSC in addition to the fault ride through capability of the inverter associated with DFIG rotor.

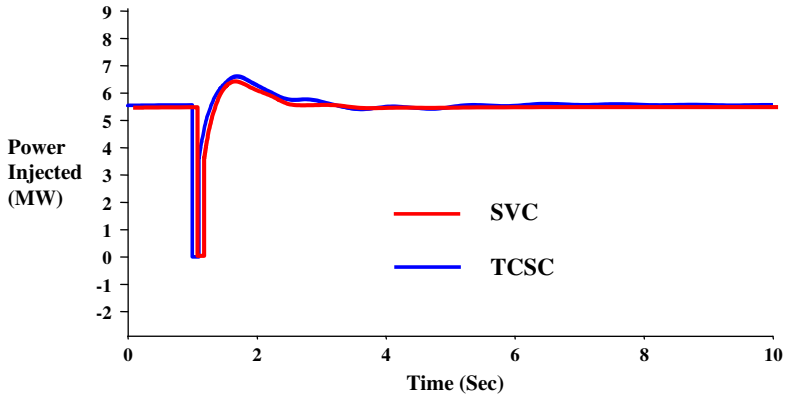

Fig. 20. Active power injected by wind farm with SVC and TCSC.

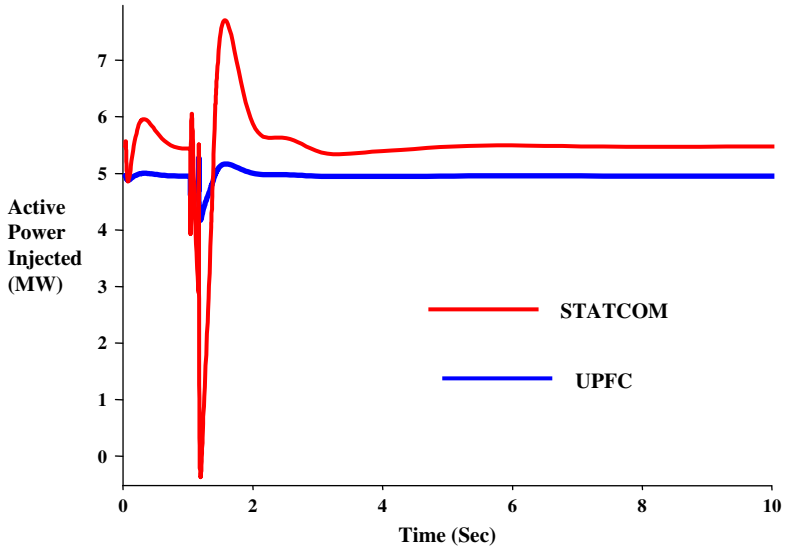

Fig. 21. Active power Injected by the wind farm with STATCOM and UPFC.

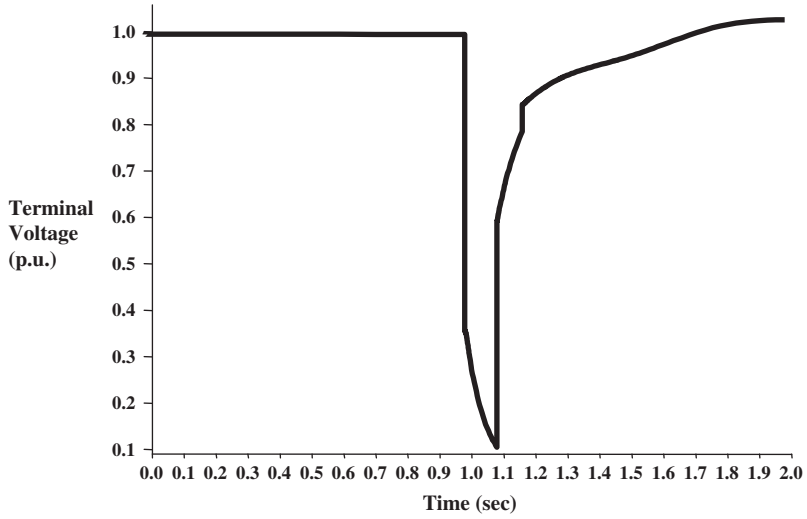

Fig. 22. Induction generator terminal voltage without FACTS.

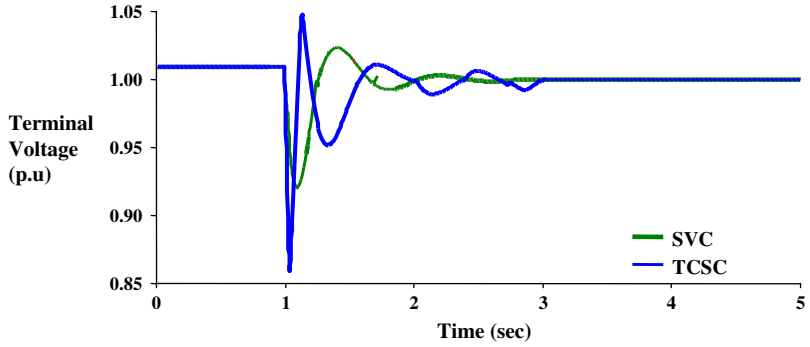

Fig. 23. Induction generator terminal voltage – Effect of SVC and TCSC.

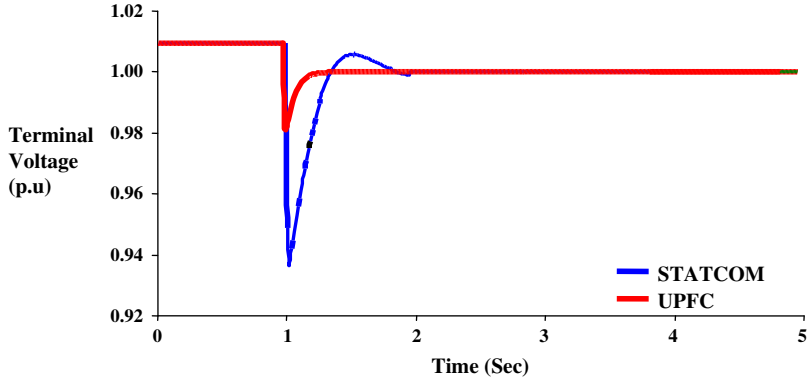

Fig. 24. Induction generator terminal voltage – Effect of STATCOM and UPFC.

Fig. 21 shows the active power injected by the wind farm following the transient fault with STATCOM/UPFC. It can be observed that due to the fast transient response of the STATCOM the active power injected comes to the steady state of 5.5 MW within 2 s. It can be observed that there are no appreciable oscillations or power fluctuations in the induction generator terminal after the disturbance. This is due to the reactive power support provided by the series converter and shunt converters of UPFC in addition to the fault ride through capabilities of the rotor side converter of DFIG.

3.4. Induction generator terminal voltage – Effect of FACTS controllers

The response in induction generator terminal voltage following the transient fault is shown in Fig. 22, without FACTS controllers in the network. The under voltage protection system associated with the wind turbine disconnects the stator from the network if the voltage at its stator terminals is less than 0.75 p.u. for a period of 0.08 s.

Figs. 23 and 24 show the response of the induction generator terminal voltage with SVC/TCSC and STATCOM/UPFC.

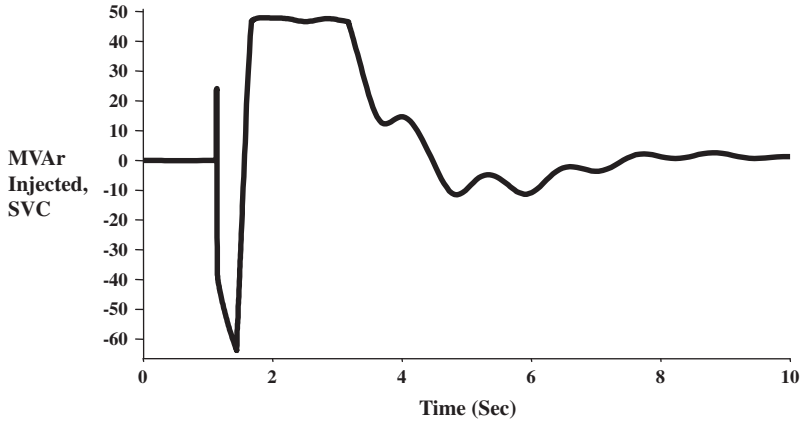

Fig. 25. Dynamic reactive compensation – SVC.

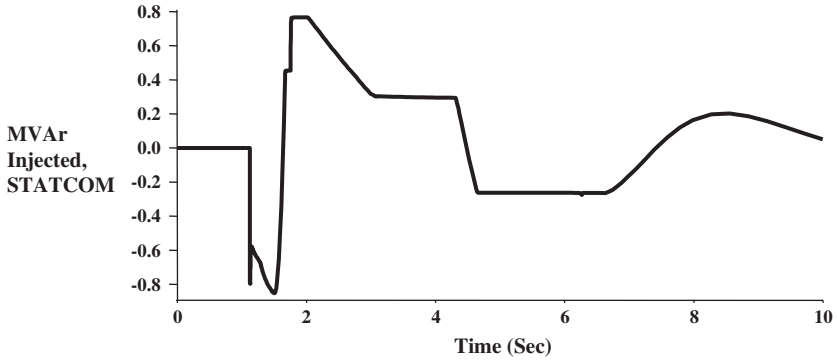

Fig. 26. Dynamic reactive compensation – STATCOM.

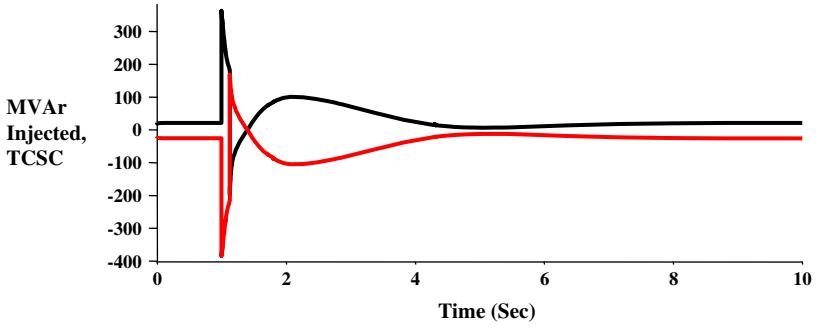

Fig. 27. Dynamic reactive compensation – TCSC.

It can be concluded that terminal voltage of the DFIG is above 0.75 p.u. after 0.1 s.

Comparing Figs. 22–24 it can be concluded that the UPFC improves the fault ride through capability of the DFIG very effectively.

3.5. Dynamic reactive compensations of the FACTS controllers

Dynamic reactive compensation of the wind farm can be organized in several ways. This depends on (i) the demand of reactive compensation for voltage reestablishing (ii) controllability of the equipment and (iii) Cost. When the success criterion is to get the voltage reestablishing within the predefined range, e.g., avoid uncontrollable as well as over-voltages in the grid, the dynamic reactive compensation can be capacitive or inductive. So long as no disconnection of the wind turbines occurs and the grid connected induction generators absorb reactive power during voltage reestablishing process, the dynamic reactive compensation should be capacitive.

The dynamic reactive compensation of the FACTS controllers, play a major key role in controlling the transients on rotor speed oscillations of the asynchronous generator.

The reactive power compensation provided by shunt FACTS Controllers are shown in Figs. 25 and 26. Comparing the figures, it can be observed that the compensation of the SVC swings from −60 MVAr to 50 MVAr for stabilizing the rotor speed oscillations. Use of an SVC with a less capacity results in uncontrollable voltage

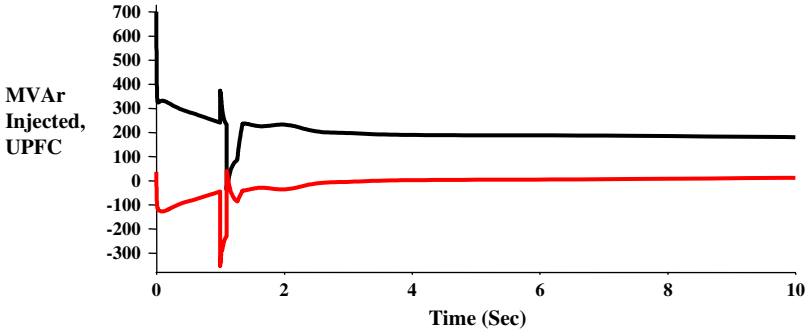

Fig. 28. Dynamic reactive compensation – UPFC.

decay or in sufficiently damped voltage oscillations. The dynamic reactive power compensation of STATCOM for achieving the same control objective is only 0.8 MVAr. Hence it can be concluded that a STATCOM is cost effective when compared to SVC for stabilizing rotor speed oscillations of the induction generator.

Figs. 27 and 28 compare the dynamic reactive compensations of TCSC and UPFC following the disturbance. From Fig. 27 it can be observed that the MVAr injected by the TCSC branch swings from its steady state value of 50–300 MVAr. It can be observed that the series converter reactive power rating of UPFC swings from 400 MVAr to 800 MVAr following the disturbance. This high transient reactive power requirement results in increased cost of series/shunt converters.

4. Results and discussion

For the simulation study the gains and time constants of the FACTS controllers are tuned using a conventional optimization program, which minimizes the voltage/rotor speed oscillations of the induction generator. From the results we conclude that among shunt connected FACTS controllers the STATCOM provides better damping the oscillations compared to that of the SVC. Also, the dynamic reactive compensation (Transient Rating) required by the STATCOM is lesser than SVC. This is due to the fact that a STATCOM is basically voltage sourced converter based shunt controller and SVC is a shunt connected thyristor switched capacitor/reactor. Among series connected FACTS controllers the UPFC damps both rotor angle oscillations of synchronous generators and rotor speed oscillations of induction generator very effectively when compared with TCSC. This is due to the reactive support provided by the shunt branch of the UPFC following the disturbance. However the reactive power rating of UPFC is very high compared to that of the TCSC. It is suggested that a STATCOM of suitable rating may be installed at the point of common coupling (PCC) with or without a capacitor may be used for stabilizing rotor speed oscillations associated with doubly fed variable speed induction generators following transient faults and disturbances.

5. Conclusion

The development of wind turbine and wind farm models is vital because as the level of wind penetration increases it poses dynamic stability problems in the power system. For the present work we have taken a doubly fed induction generator model and illustrated the presence of sustained oscillations with wind farms. Suitable Flexible AC Transmission Systems controllers are modeled using the non-linear simulation models and the transient ratings of the FACTS controller are obtained to stabilize the rotor speed/rotor angle oscillations in a DFIG based wind energy conversion scheme. The rotor speed stability of the DFIG based system following a generator outage is studied. It can be observed that the effect of low voltage ride through (LVRT) is very minimum following the contingency and the presence of a FACTS device like the SVC improves the rotor speed stability.

Acknowledgements

The first author (Dr. N. Senthil Kumar) would like to thank his father Mr. S.K. Natarajan and wife Mrs. Bhuvana who consistently supported and encouraged him a lot during his research work morally.

Appendix A. Doubly fed induction generator dynamic data

A.1. Parameters

Base values for the per unit system conversion.
Base power: 100 MVA
Base voltage: 0.69 kV for low voltage bus bar, 150 kV for high voltage busbar.

B. Line data

From	To	R	X	Transformer tap
1	2	0.000185	0.00769	1.0526
2	3	0.00208	0.02285	–
2	3(2)	0.00208	0.02285	–
3	4	0.00208	0.02285	–
3	5	0.00185	0.00769	–

Load data

Load bus	P_D (MW)	Q_D (MVAr)
4	5000	2000
5	500	175

Appendix B. Dynamic data of generators

B.1. Doubly fed induction generator

Rated apparent power MVA: 20 MVA.
Rotor inertia: 3.527 MW s/MVA.
R_s (p.u.) = 0.0693.
X_s (p.u.) = 0.080823.

R_r (p.u.) = 0.00906.
X_r (p.u) = 0.09935.
X_m (p.u.) = 3.29.
Rotor speed for synchronization: 0.9 p.u.
Minimum rotor speed: 0.56 p.u.
Maximum rotor speed: 1.122 p.u.

B.2. Gains of FACTS controllers

	Gain parameters	Tuned gains
SVC	*K*	48.2
STATCOM	*K*	47.3
TCSC	*K*	41.1
UPFC	*K*	40

References

[1] Kundur. Power system stability and control. New York: McGraw Hill; 1994.
[2] Chompoo-inwai Chai, Lee Wei-Jen, Fuangfoo Pradit, Williams Mitch, Liao James R. System impact study for the interconnection of wind generation and utility system. IEEE Trans Ind Appl 2005;41(1):163–8.
[3] Abdel-Magid YL, El-Amin IM. Dynamic stability of wind – turbine generators under widely varying loading conditions. Int J Electric Power Energy Syst 1987;9(3):180–8.
[4] Jauch Clemens, Sorensen Poul, Norheim Ian, Rasmussen Carsten. Simulation of the impact of wind power on the transient fault behavior of the nordic power system. Electric Power Syst Res 2007;77:35–144.
[5] Samuelsson Olof, Lindahl Sture. On speed stability. IEEE Trans Power Syst 2005;20(2):1179–80.
[6] Slootweg JG, Kling WL. The impact of large scale wind power generation on power system oscillations. Int J Electric Power Syst Res 2003;67(1):9–20.
[7] Erlich Istvan, Kretschmann Jorg, Fortmann Jens, Mueller-Engelhardt Stephan, Wrede Holger. Modeling of wind turbines based on doubly fed induction generators for power system stability studies. IEEE Trans Power Syst 2007;22(3):909–19.
[8] Varma Rajiv K, Sidhu Tejbir S. Bibliographic review of FACTS and HVDC applications in wind power systems. Int J Emerging Electric Power Syst 2006;7(3):1–16.
[9] Muyeen SM, Rion Takahashi, Toshiaki Murata, Junji Tamura, Mohd. Hasan Ali. Application of STATCOM/BESS for wind power smoothening and hydrogen generation. Int J Electric Power Syst Res 79(2):365–73.
[10] Akhmatov Vladislav, Knudsen Hans, Nielsen Arne Hejde, Pedersen Jørgen Kaas, Poulsen Niels Kjølstad. Modelling and transient stability of large wind farms. Int J Electric Power Energy Syst 2003;25(2):123–44.
[11] Hansen Anca D, Michalke Gabriele. Fault ride through capability of DFIG wind turbines. Int J Renew Energy 2007;32:1594–610.
[12] EUROSTAG Release 4.3. Tractebel engineering, package documentation part 1, 2 and 3; 2004.
[13] Slootweg JG, Polinder H, King WL. Dynamic modeling of a wind turbine with a doubly fed induction generator. IEEE Power Eng Soc Meet 2001;1:644–9.
[14] Anderson, Fouad. Power system control and stability. IEEE Press Power Eng Ser.
[15] Canizares Claudio A, Pozzi Massimo, Corsi Sandro, Uzunovic Edvina. Statcom modeling for voltage and angle stability studies. Int J Electric Power Energy Syst 2003;25(6):431–41.
[16] Mohan Mathur R, Varma Rajiv K. Thyristor based FACTS controllers. IEEE Press; 2000.

Dr. N. Senthil Kumar is presently working as an assistant professor (selection grade) in the Department of Electrical and Electronics Engineering at B.S. Abdur Rahman University. His area of research includes modeling of FACTS devices for power system stability studies. Modeling of wind energy conversion systems for power system stability analysis.

Mr. J. Gokulakrishnan is a post graduate student in M.E. (Power System Engineering) in the Department of Electrical and Electronics Engineering in B.S. Abdur Rahman University.